Journal of Electron Spectroscopy and Related Phenomena 196 (2014) 142–145

Contents lists available at ScienceDirect

Journal of Electron Spectroscopy and Related Phenomena

journal homepage: www.elsevier.com/locate/elspec

Low-energy electron energy losses and inelastic mean free paths in zinc, selenium, and zinc selenide

J.D. Bourke, C.T. Chantler*

School of Physics, University of Melbourne, Parkville, Vic 3010, Australia

ARTICLE INFO

Article history:
Available online 20 February 2014

Keywords:
Electron energy loss function
Inelastic mean free paths
Electron transport
Density functional theory

ABSTRACT

We compute low-energy optical energy loss spectra for the elemental solids zinc and selenium, and for the binary compound zinc selenide. The optical data are transformed via a constrained partial-pole algorithm to produce momentum-dependent electron energy loss spectra and electron inelastic mean free paths. This enables a comparison between the electron scattering behaviour in a compound solid and its constituent elements. Results cannot be explained by aggregation methods or commonly used universal curves, and prove that new approaches are required. Our work demonstrates new capabilities for the determination of fundamental material properties for a range of structures previously inaccessible to established theoretical models, and at energy levels inaccessible to most experimental techniques.

1. Introduction

The electron inelastic mean free path (IMFP) is one of the most fundamental parameters describing electron transport in a material. It defines the mean distance travelled by an electron between successive inelastic collisions, and is crucial for quantitative analysis of a variety of spectroscopic and imaging tools such as electron energy loss spectroscopy (EELS), auger electron spectroscopy (AES), elastic peak electron spectroscopy (EPES), and electron microscopy. A strong body of literature exists, particularly from the last 35 years, following the development of theoretical models used in the determination of IMFPs in elemental solids [1–4], and tabulations are available across a broad energy range, typically from 50 eV to 30 keV [5].

Recent experimental work, however, has raised questions about the accuracy of these tabulations in the low energy regime, particularly below around 120 eV [6–8]. Few tabulations quote any data at all below 50 eV – an important region dominated by plasmon excitations that has particularly significant effects on structural analysis tools such as X-ray absorption fine structure (XAFS) analysis [9] and low energy electron diffraction (LEED) [10]. Further, information regarding IMFPs in compound structures generally must be inferred from elemental tables following universal curves or aggregation techniques [11].

These problems are largely due to difficulties in accurately quantifying the optical energy loss function (ELF) for a material in the low energy region. The ELF may be interpreted physically as the relative probability of a material accepting an electronic excitation with a given energy $\hbar\omega$ and momentum $\hbar q$, and is expressed in terms of the complex dielectric function $\epsilon(q,\omega)=\epsilon_1(q,\omega)+i\epsilon_2(q,\omega)$ following

$$\mathrm{ELF} = \mathrm{Im}\left[\frac{-1}{\epsilon(q,\omega)}\right] = \frac{\epsilon_2(q,\omega)}{\epsilon_1(q,\omega)^2+\epsilon_2(q,\omega)^2} \quad (1)$$

This quantity is not to be confused with the energy loss spectrum, which describes the response of the incoming particle, rather than the response of the absorbing/scattering material. The ELF is said to be the optical ELF in the limit $q \to 0$, due to the small momentum supplied by a photon relative to an energetic electron. Modern theories, including the full Penn algorithm [5], partial pole models [12], and self-energy/Green's function approaches [13] all rely on transforms of the optical ELF in order to estimate the IMFP.

Optical ELF data used in IMFP calculations have previously been sourced almost exclusively from experimental data, with the optical transmission and reflection measurements of Hagemann et al. [14] and the exhaustive compilation of Palik [15] being most commonly cited. In recent times REELS measurements have also provided experimental optical ELFs, which have sometimes shown significant disagreements with the aforementioned tabulated data [16].

These tabulations are often inconsistent, do not typically provide uncertainties, and do not generally cover all elemental solids, let alone any useful range of compounds. It is therefore

* Corresponding author. Tel.: +61 3 83445437; fax: +61 3 93474783.
E-mail address: chantler@unimelb.edu.au (C.T. Chantler).

http://dx.doi.org/10.1016/j.elspec.2014.02.004
0368-2048/

essential that a theoretical framework be defined in order to provide a generalised approach to optical ELF, and subsequent IMFP, determination. We have made developments in the application of density functional theory (DFT), which enables calculations of a range of optical properties at low excitation energies for periodic systems [16]. In this work we utilise those developments in a study of the binary compound zinc selenide, enabling not only the first ever published determination of the IMFP of ZnSe, but also an analysis of the relationship between the optical and electron energy loss properties of a binary material and those of its constituent elements. This allows us to critically investigate longstanding assumptions regarding the aggregation of IMFPs for compounds and mixtures, and demonstrates the value of a purely theoretical approach for the detailed study of a more general class of materials.

2. Theory

The optical dielectric function for a material with complex band structure, such as a periodic solid, is commonly expressed as a summation of terms corresponding to the dielectric response of an ensemble of nearly-free electron gases. The basic theory for the quantum-mechanical free-electron gas is given by Lindhard [17]. One can utilise Lindhard dielectric functions to construct the solid-state optical dielectric function following [18]

$$\epsilon(0,\omega) = 1 + \lim_{q\to 0}\frac{4\pi\mathbf{e}^2}{q^2}\sum_{n,n',\mathbf{k}}\frac{f^0(\mathbf{k}) - f^0(\mathbf{k}+\mathbf{q})}{E_{n'}(\mathbf{k}+\mathbf{q}) - E_n(\mathbf{k}) - \hbar\omega}|M_{n,n'}(\mathbf{k},\mathbf{q})|^2 \tag{2}$$

where the Lindhard expressions, characterised in terms of the Fermi distribution f_0, are modulated by a series of transition matrix elements $M_{n,n'}(k, q)$. These terms can be expressed approximately as

$$M_{n',n}(\mathbf{k},\mathbf{q}) = \langle n', \mathbf{k}|e^{-i\mathbf{q}\cdot\mathbf{r}}|n, \mathbf{k}+\mathbf{q}\rangle \tag{3}$$

The detailed procedure for the evaluation of Eq. (2) has been developed by Ambrosch-Draxl and Sofo [18] and implemented into a module for the band structure package WIEN2k [19]. WIEN2k utilises a self-consistent field algorithm to determine electron eigenstates $|n, \mathbf{k}\rangle$ for periodic structures following a linearised augmented plane-wave (LAPW) implementation of Kohn–Sham DFT. The Kohn–Sham equation is given by

$$\left(-\frac{\hbar}{2m}\nabla^2 + V_{Ne} + V_{ee} + V_{xc}\right)\psi = E\psi \tag{4}$$

where the potential components correspond to the nuclear–electron interactions (V_{Ne}), electron–electron interactions (V_{ee}), and exchange and correlation (V_{xc}). These components can be evaluated as functions of local electron densities, alleviating the need for consideration of pair-wise electron interactions – an intractable problem for a solid.

With this framework in place one can determine the optical dielectric function $\epsilon(0, \omega)$ and consequently the optical ELF $\mathrm{Im}[-1/(\epsilon(0, \omega))]$. As mentioned, the transformation of the optical ELF is critical for the evaluation of the electron IMFP. Here we utilise a partial pole transformation [12], which utilises the natural q-dependence of the Lindhard theory to obtain the momentum-dependent ELF $\mathrm{Im}[-1/(\epsilon(q, \omega))]$. To wit:

$$\mathrm{Im}\left[\frac{-1}{\epsilon(q,\omega)}\right] = \sum_i A_i \mathrm{Im}\left[\frac{-1}{\epsilon_L(q,\omega;\omega_p=\omega_i)}\right] \tag{5}$$

where $\epsilon_L(q, \omega)$ is the Lindhard dielectric function. The principal defining parameter for a Lindhard function is the plasma frequency ω_p which, in the partial pole model, may take on a number of values ω_i resulting from the different local free-electron gas densities that are considered to make up the scattering material. The relative amplitudes of the Lindhard terms at different plasma frequencies are given as A_i, and these may be evaluated using the requirement that the momentum-dependent ELF matches that calculated in the optical limit via DFT:

$$\mathrm{Im}\left[\frac{-1}{\epsilon_{\mathrm{DFT}}(0,\omega)}\right] = \sum_i A_i \mathrm{Im}\left[\frac{-1}{\epsilon_L(0,\omega;\omega_p=\omega_i)}\right] \tag{6}$$

Since the Lindhard dielectric function leads to delta function components in the optical ELF, this criterion is straightforward to fulfil by allocating closely spaced, periodic ω_i values and defining the amplitude parameters A_i following

$$\mathrm{Im}\left[\frac{-1}{\epsilon_{\mathrm{DFT}}(0,\omega)}\right] = \sum_i \frac{A_i\pi}{2\omega}\delta(\omega-\omega_i) \tag{7}$$

This enables us to build a complete electron ELF $\mathrm{Im}[-1/(\epsilon(q, \omega))]$. Recalling that this function is interpreted physically as a relative probability of an excitation occurring in the scattering material, we express the electron IMFP in terms of the ELF following the well-known relation [3]:

$$\lambda^{-1}(E) = \frac{\hbar}{a_0\pi E}\int_0^{((E-E_F)/\hbar)}\int_{q_-}^{q_+}\frac{1}{q}\mathrm{Im}\left[\frac{-1}{\epsilon(q,\omega)}\right]dq\,d\omega \tag{8}$$

The limits of integration for the momentum transfer, $q_\pm$, are given by

$$q_\pm = \sqrt{\frac{2mE}{\hbar^2}} \pm \sqrt{\frac{2m}{\hbar^2}(E-\hbar\omega)} \tag{9}$$

following kinematic requirements with respect to the energy transfer of the incoming electron.

3. Results

We first examine, in Fig. 1, the optical ELFs determined via DFT for zinc, selenium, and zinc selenide. We note that the optical response of solids is often highly dependent on the crystal or molecular structure, and that the crystal systems of these three materials - hexagonal for zinc, trigonal for (grey) selenium, and cubic zincblende for zinc selenide – are highly varied.

Despite these variations, we are surprised to find that the optical ELF of ZnSe is qualitatively representative of an aggregate of the responses of Zn and Se. Specifically, while the main feature of the Zn loss function is a clear double-peak at 13 eV and 19 eV, and the Se spectrum exhibits a well-defined single peak at 20 eV, the ZnSe

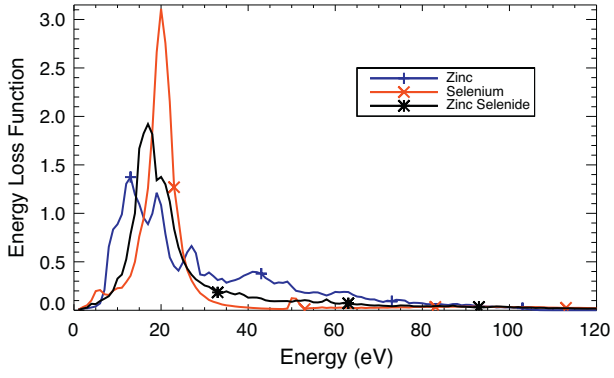

Fig. 1. Optical energy loss functions of zinc, selenium, and zinc selenide determined using the WIEN2k implementation of density functional theory. Despite substantial structural differences between the three materials, the major peak of ZnSe is qualitatively similar to the aggregate heights, widths, and energy positions of the major peaks associated with its component elements.

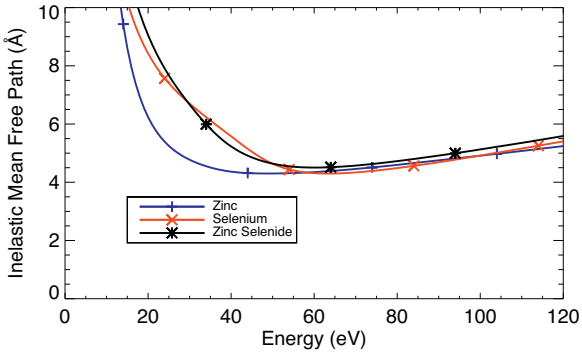

Fig. 2. Electron inelastic mean free paths for zinc, selenium, and zinc selenide, determined from a partial pole representation of the optical loss spectra shown in Fig. 1. Despite the appearance of the optical energy loss function of zinc selenide, its IMFP appears to much more closely resemble that of selenium than of zinc.

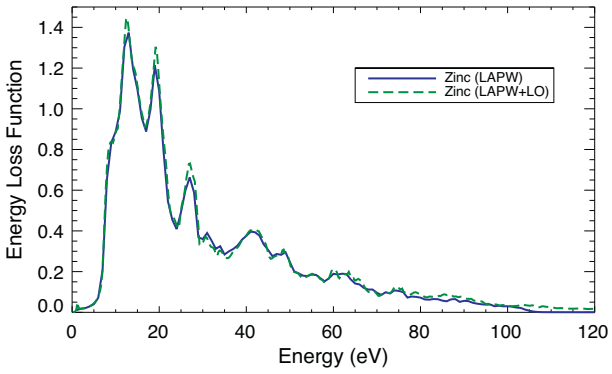

Fig. 3. Optical energy loss function of zinc calculated using density functional theory via the standard LAPW basis set, in addition to an expanded basis including local orbitals (LAPW+LO). The addition of LOs typically results in increased loss magnitudes for energies beyond 10–20 eV, with the effect increasing in significance at greater energies.

spectrum has a strong intermediate peak at 17 eV with a suppressed secondary peak at 20 eV. The prominent loss region from ZnSe also possesses an aggregated width between those of Zn and Se, and an intermediate peak height.

The ZnSe spectrum does not reproduce the smaller peaks and structures seen at higher energies for Zn and Se, however it generally runs at a magnitude between the two – even crossing the spectra at the same energy. These observations could easily lead to the suggestion that, crystal structure aside, an aggregation technique would be appropriate in the determination of ZnSe loss data and the electron IMFP in the absence of a robust theoretical framework, from known data of its constituent elements.

Transforms to predict the IMFP, however, prove that such an understanding would be incorrect. Fig. 2 shows the IMFPs for Zn, Se, and ZnSe calculated using the partial pole framework discussed in the previous section. Far from being a weighted mean of its component parts, the IMFP of ZnSe appears much more closely related to that of Se.

Such a result is surprising given the forms of the optical ELFs, and is difficult to explain phenomenologically. One may, however, point to the range of q-integration defining the IMFP from Eq. (9), which exaggerates the contribution from low-energy components in the ELF. This, at least, would explain why Zn possesses a characteristically lower IMFP at low energies, as it also has a major loss peak at a lower energy than either Se or ZnSe.

A more surprising and less readily explained feature of Fig. 2, however, is that for the majority of the range we have considered (and likely for higher energies as well), the IMFP of ZnSe is higher than that of *both* Zn and Se. No form of aggregation could predict such an outcome, and the result is clearly counter-intuitive. This demonstrates that a detailed theoretical modelling of the electronic structure of each material is necessary to produce a realistic energy loss spectrum and consequent electron IMFP.

The use of DFT for the calculation of optical data is a new development over the last few years and is subject to computational difficulties at increasing energies. As this is one of the highest-energy calculations of the optical ELF reported using DFT, we briefly address the issue of semi-core and continuum states, which should increasingly impact upon the high-energy region of the optical ELF, but may be poorly described by the standard LAPW basis set [20,21]. It is commonly suggested that the description of these states be improved by the introduction of local orbitals (LOs) whose values reduce to zero beyond the muffin-tin regions. In Fig. 3 we demonstrate the effect of introducing such orbitals into the calculation for the optical ELF of Zn, which is denoted as a LAPW+LO calculation.

We see that the magnitude of the loss spectrum increases, particularly at major peaks, above around 12 eV due to the inclusion of the LOs. The increase becomes particularly significant beyond 100 eV. This is qualitatively consistent with results seen by other authors [22,20], although others have observed greater effects than are seen here. The inclusion of LOs is subject to free parameters governing the states to be described, and the convergence criteria of the calculation is significantly affected in terms of the number of plane waves and the muffin-tin radius. Our result applies the same computational parameters for both the LAPW and LAPW+LO bases where possible. The differences in ELF are sufficiently small to not alter our conclusions regarding the IMFP, particularly in light of the relatively weak IMFP dependence on high-energy ELF behaviour. These considerations would become far more significant, however, if the DFT calculations were expanded to significantly higher energies.

Prior to the development of DFT methods for calculating optical ELFs, those wishing to obtain IMFP data for compounds such as ZnSe, or even relatively unstudied elements such as Zn and Se, were required to utilise predictive formulae, or universal curves, based on empirical fitting to compilations of known IMFPs for other materials. The most widely used of these, the TPP-2M equation [23], includes material parameters such as atomic mass, density, valence number, and bulk plasma frequency in order to impart some physical basis for the calculated IMFP. In Fig. 4 we plot our own results for the IMFPs of Zn, Se, and ZnSe alongside those determined via the TPP-2M equation for energies in excess of 50 eV.

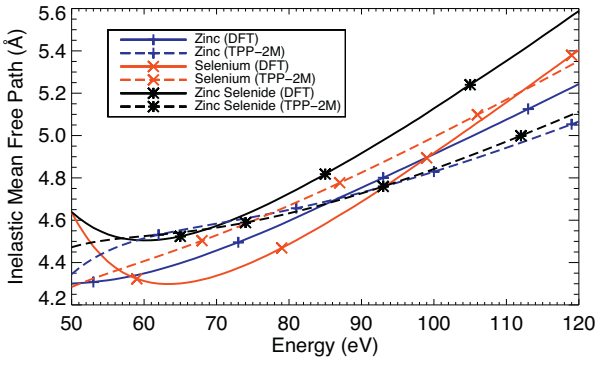

Fig. 4. Electron inelastic mean free paths for zinc, selenium, and zinc selenide. Solid lines indicate calculations made via a partial pole extension to optical ELF data from DFT, while dashed lines are obtained using the empirical predictive formula known as TPP-2M. No consistency is seen between results from the same materials, nor is the relationship between ZnSe and its constituent elements consistent between the two approaches. The data from TPP-2M extends to higher energies but cannot be meaningfully extrapolated below 50 eV.

There is no consistency between our results and those of the predictive formula for any of the materials studied. Given that the predictive formula is both empirical and designed for use at higher energies (the TPP-2M equation does not produce meaningful results below 50 eV), there is little to infer from such a result. A previous analysis by Tanuma et al. of an alternative predictive formula, given by Gries [24], also demonstrated inconsistency with IMFPs from calculations using optical data modelling, albeit at much higher energies [25]. The relationship between the IMFP of ZnSe with those of its constituent elements, however, is clear. While the theory developed here predicts a significantly higher IMFP for ZnSe than for Zn and Se in the 50–120 eV range, and a relative consistency of IMFPs between ZnSe and Se overall, the TPP-2M predictive formula instead suggests a strong correlation between the IMFPs of ZnSe and Zn. We believe this result to be primarily due to the exaggerated importance of valence number in the TPP-2M fitting, physically justified by the dominant contribution of valence electrons to low-energy electron scattering. However, an accurate and quantitative account of inelastic scattering parameters, particularly in the regions studied here, ultimately demands explicit consideration of the complex band structure of a material, which is afforded for the first time theoretically via the DFT determination of the optical ELF.

4. Discussion

This study presents new ELF and IMFP data for Zn, Se, and ZnSe – the latter two having had no such data previously available in the literature. The IMFP for Zn has only been physically quantified previously in recent work by Werner et al. [16], who also utilise DFT to calculate the optical ELF, in addition to REELS experiments. Their IMFP results from both sources of optical data are relatively consistent with our own, deviating by only 2.0–2.5% between 100 eV and 120 eV. Further data for Zn, Se, and ZnSe may soon also be inferred experimentally in forthcoming analysis of X-ray absorption data taken using the X-ray extended range technique [26,27], following an extraction algorithm previously applied to copper and molybdenum [6,7].

Our results demonstrate the applicability of modern toolsets for examining materials that have hitherto been either unreachable by theoretical approaches, or too cumbersome to tackle experimentally. The need for IMFP data for a wide range of materials, far beyond the elemental solids and small subset of common compounds currently tabulated, is evidenced most strongly by the many thousands of citations still being made to works espousing predictive formulae or universal curves. The developments discussed in this work will enable a significant portion of analyses that utilise such data to finally treat with physical parameters rather than empirical ones.

We have demonstrated a sample of the level of variability between a physical approach and one based on universal fitting. It is reasonable to suggest that in many cases the discrepancies between such approaches may be significantly higher. Even more importantly, we have demonstrated an approach applicable to energies below the 50 eV threshold, a critical area for analysis in a number of fields such as XAFS, EELS, and LEED.

These developments are not all-encompassing. Limitations still exist, particularly with respect to the applicability of DFT to higher electron energies, and the assumption of periodicity in the modelling of the solid-state band structure. It is apparent that further work is invited for cluster materials such as isolated molecules, catalytic centres, amorphous and nano-materials – particularly in light of their strong interest to the XAFS community [28,29]. This work impacts strongly upon such considerations, as we have made useful observations regarding the contribution of constituent atoms to the optical ELF and IMFP of compound materials. It is apparent from this limited case that any aggregation of contributions from elemental components, whether weighted by local electron density, relative volume, or valence contribution, would be a poor metric for accurate IMFP determination. Our current example has suggested that an aggregation technique may be more applicable in the ELF regime, however further investigation is warranted to ascertain the extent to which this behaviour is seen in other systems. Such an approximation, if reasonable, could still be useful for IMFP evaluation in systems inaccessible to DFT modelling.

The DFT approach to ELF calculation, coupled with a rigorous and well-constrained extension to quantify electron energy losses, has potential to aid in the understanding of how fundamental material parameters impact on both optical and electronic scattering values. It allows detailed and wide-ranging investigations of the effects of small variations in crystal structures, bond lengths, and other considerations such as the presence of impurities or polarisation effects. The directional dependence of the scattering response of a material may also be probed via specific consideration of the dielectric function as a tensor quantity – an approach already facilitated by DFT. These new techniques for theoretical IMFP investigation will have significant consequences for the analysis of a wide-range of experimental techniques involving periodic compounds, and will increase the information content available from the many experimental interrogations that utilise low-energy electrons as a probe.

Acknowledgements

The authors acknowledge the helpful contributions of Nick Rae, the team at Melbourne, and the ANBF, APS, and AS grants that have assisted in the development of this research.

References

[1] C.J. Tung, J.C. Ashley, R.H. Ritchie, Surf. Sci. 81 (1979) 427.
[2] D.R. Penn, Phys. Rev. B 35 (1987) 482.
[3] S. Tanuma, C.J. Powell, D.R. Penn, Surf. Interface Anal. 17 (1991) 911.
[4] C.J. Powell, A. Jablonski, J. Phys. Chem. Ref. Data 28 (1999) 19.
[5] S. Tanuma, C.J. Powell, D.R. Penn, Surf. Interface Anal. 43 (2011) 689.
[6] J.D. Bourke, C.T. Chantler, Phys. Rev. Lett. 104 (2010) 206601.
[7] C.T. Chantler, J.D. Bourke, J. Phys. Chem. Lett. 1 (2010) 2422.
[8] R. Zdyb, T.O. Mentes, A. Locatelli, M.A. Nino, E. Bauer, Phys. Rev. B 87 (2013) 075436.
[9] J.D. Bourke, C.T. Chantler, Nucl. Instrum. Methods A 619 (2010) 33.
[10] J. Rundgren, Phys. Rev. B 59 (1999) 5106.
[11] C.J. Powell, J. Electron Spectrosc. 47 (1988) 197.
[12] J.D. Bourke, C.T. Chantler, J. Phys. Chem. A 116 (2012) 3202.
[13] A.P. Sorini, J.J. Kas, J.J. Rehr, M.P. Prange, Z.H. Levine, Phys. Rev. B 74 (2008) 165111.
[14] H.-J. Hagemann, W. Gudat, C. Kunz, Deutsches Elektronensynchrotron Report SR-74/7 (unpublished).
[15] E.D. Palik, Handbook of Optical Constants of Solids III, Academic Press, New York, 1998.
[16] W.S.M. Werner, K. Glantschnig, C. Ambrosch-Draxl, J. Phys. Chem. Ref. Data 38 (2009) 1013.
[17] J. Lindhard, Dan. Mat. Fys. Medd. 28 (1954).
[18] C. Ambrosch-Draxl, J.O. Sofo, Comput. Phys. Commun. 175 (2006) 1.
[19] P. Blaha, K. Schwarz, G.K.H. Madsen, D. Kvasnicka, J. Luitz, WIEN2k – An Augmented Plane Wave Plus Local Orbitals Program for Calculating Crystal Properties, Vienna University of Technology, Austria, 2014.
[20] P.L. Potapov, K. Jorissen, D. Schryvers, D. Lamoen, Phys. Rev. B 70 (2004) 045106.
[21] D. Singh, Phys. Rev. B 43 (1991) 6388.
[22] C. Hebert, Micron 38 (2007) 12.
[23] S. Tanuma, C.J. Powell, D.R. Penn, Surf. Interface Anal. 21 (1993) 165.
[24] W.H. Gries, Surf. Interface Anal. 24 (1996) 38.
[25] S. Tanuma, C.J. Powell, D.R. Penn, Surf. Interface Anal. 25 (1997) 25.
[26] N.A. Rae, C.T. Chantler, Z. Barnea, M.D. de Jonge, C.Q. Tran, J.R. Hester, Phys. Rev. A 81 (2010) 022904.
[27] C.T. Chantler, Eur. Phys. J. Spec. Top. 169 (2009) 147.
[28] J.L. Glover, C.T. Chantler, A.V. Soldatov, G. Smolentsev, M.C. Feiters, AIP Conf. Proc. 882 (2007) 625–627.
[29] C.T. Chantler, N.A. Rae, M.T. Islam, S.P. Best, J. Yeo, L.F. Smale, J. Hester, N. Mohammadi, F. Wang, J. Synch. Radiat. 19 (2012) 145.